Accuracy assessment of repeat-pass radar interferometry for topographic mapping and deformation analysis

Ramon Hanssen and Roland Klees

DEOS, Delft University of Technology
Delft, The Netherlands

email: hanssen@geo.tudelft.nl
klees@geo.tudelft.nl

1. Problem definition

Repeat-pass radar interferometry can be used for the recovery of topography or surface deformation on earth from random interferometric phase observations φ_k, with $k = i + (i-1)j$, where i and j represent the row and column of the interferogram, respectively. For every observation, at least five unknown parameters need to be estimated:

- topographic height H_k,
- deformation in slant direction D_k
- slant atmospheric delay during acquisition 1: $S_k^{t_1}$,
- slant atmospheric delay during acquisition 2: $S_k^{t_2}$, and
- integer ambiguity number w_k.

Therefore, the problem is ill-posed and underdetermined. The observed phase values φ_k form a real stochastic vector of observations $\boldsymbol{\varphi} \in \mathbb{R}^n$. After linearization the relation between the observations and the unknown parameters can be written as a Gauss-Markoff model with $E\{\boldsymbol{\varphi}\} = \mathbf{A}\mathbf{x}$; and $D\{\boldsymbol{\varphi}\} = \mathbf{C}_{\boldsymbol{\varphi}} = \sigma^2\mathbf{Q}_{\boldsymbol{\varphi}}$ where $\mathbf{A}$ is the design matrix, $\mathbf{C}_{\boldsymbol{\varphi}}$ is the variance-covariance matrix, $\mathbf{Q}_{\boldsymbol{\varphi}} \in \mathbb{R}^{n\times n}$ the real positive-semidefinite $n \times n$ cofactor matrix, and $\sigma^2 \in \mathbb{R}^+$ the a priori variance factor. The vector of parameters $\mathbf{x} \in \mathbb{R}^{5n}$ is assumed to be real and non-stochastic.

Tailoring the model for repeat-pass interferometry we can write the system of linearized observation equations, or *functional model* as

$$E\{\begin{bmatrix}\varphi_1\\ \varphi_2\\ \vdots\\ \varphi_n\end{bmatrix}\} = \begin{bmatrix}\mathbf{A}_1 & & & \\ & \mathbf{A}_2 & & \\ & & \ddots & \\ & & & \mathbf{A}_n\end{bmatrix}\begin{bmatrix}\mathbf{x}_1\\ \mathbf{x}_2\\ \mathbf{x}_3\\ \vdots\\ \mathbf{x}_n\end{bmatrix} \qquad (1)$$

where $\mathbf{A}_k$ is the part of the design matrix corresponding to observation k, defined as:

$$\mathbf{A}_k = \begin{bmatrix}\frac{4\pi}{\lambda}\frac{R_k \sin\theta_k}{B_k^{\perp}}, & \frac{4\pi}{\lambda}, & \frac{4\pi}{\lambda}, & -\frac{4\pi}{\lambda}, & -2\pi\end{bmatrix}, \qquad (2)$$

and the parameter vector $\mathbf{x}_k$ corresponding to observation k is:

$$\mathbf{x}_k = \begin{bmatrix}H_k, & D_k, & S_k^{t_1}, & S_k^{t_2}, & w_k\end{bmatrix}^T. \qquad (3)$$

The dispersion of the vector of observations can be estimated using empirical coherence measurements or system theoretical considerations, and the diagonal variance-covariance matrix $\mathbf{C}_{\boldsymbol{\varphi}}$ can be written as:

$$\mathbf{C}_{\boldsymbol{\varphi}} = \begin{bmatrix}\sigma_1^2 & & & \\ & \sigma_2^2 & & \\ & & \ddots & \\ & & & \sigma_n^2\end{bmatrix} = \sigma^2\mathbf{Q}_{\boldsymbol{\varphi}}, \quad (\sigma^2 = 1), \qquad (4)$$

where σ_k^2 can be approximated using the estimated coherence values from the coregistered SAR data.

Design matrix $\mathbf{A}$ has a rank defect of $4n$. To solve this problem, we assume that either topography H_k, or deformation D_k are known, depending on the application. Moreover, we assume that the integer ambiguity number w_k is known as well, i.e., phase unwrapping can be performed perfectly. Nonetheless, both assumptions can only reduce the rank deficiency from $4n$ to $2n$, which makes the system still not solvable. Therefore, we propose to rephrase the model by lumping the atmospheric slant delay signal into one parameter $S_k = S_k^{t_1} - S_k^{t_2}$, transferring this parameter to the stochastic model and replace $\mathbf{C}_{\boldsymbol{\varphi}}$ by

$$\mathbf{C} = \mathbf{C}_{\boldsymbol{\varphi}} + \mathbf{C}_{\mathbf{s}}, \qquad (5)$$

where $\mathbf{C}_{\mathbf{s}}$ is the variance-covariance matrix of the atmospheric delay parameter S_k. Using this approach, the design matrix $\mathbf{A}$ has full rank. Proper definition of $\mathbf{C}$ in terms of measurement noise and atmospheric noise provides the necessary tools for data adjustment and filtering. Here, the characteristics of the atmospheric error signal is discussed.

2. Atmospheric error signal

The influence of the refractivity distribution in the atmosphere is apparent in two distinct phenomena: vertical stratification and turbulent mixing. In the sequel, the influence of both phenomena is discussed.

2.1 Error due to vertical stratification

Fig. 1 shows a sketch of two different vertical refractivity N_{t_i} profiles and their effect on two points on an imaginary mountain, p and q.

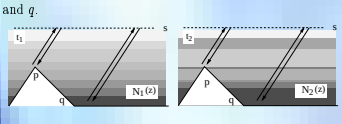

Fig. 1. Different vertical stratification of refractivity N during the two acquisitions.

In terms of cumulative delay δ, the rays to point q at the surface during the two acquisitions are sketched in Fig. 2. The observed

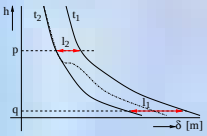

Fig. 2. Sketch of the cumulative delay curves during the two acquisitions.

delay between the two points in the interferogram, D_{pq}, due to the vertical stratification, can be written as:

$$\begin{aligned} D_{pq} &= (\delta_q^{t_1} - \delta_p^{t_1}) - (\delta_q^{t_2} - \delta_p^{t_2}) \\ &= (\delta_q^{t_1} - \delta_q^{t_2}) - (\delta_p^{t_1} - \delta_p^{t_2}) \\ &= l_2 - l_1, \end{aligned} \qquad (6)$$

in other words, the observed phase error in the interferogram between point p and q is only due to the difference in the cumulative delay values at both altitudes. As the whole refractivity profile is needed to calculate the cumulative delay, it is not possible to determine the phase error based on surface meteorological information alone. As an example, a cloud layer in between point p and q would not be noticed in the surface data, whereas it could shift the cumulative delay noticably, as indicated by the dotted line in Fig. 2.

To study the variability of the refractivity profiles, 365 radio sonde profiles acquired daily at noon during 1998 in the Netherlands, have been analyzed. The refractivity values, or delay values in ppm, are shown in Fig. 3. Using this data set, it is

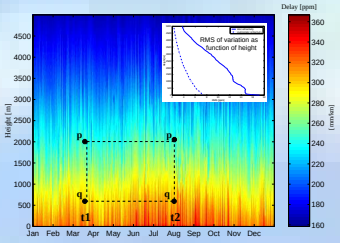

Fig. 3. 365 refractivity profiles obtained from radio sonde observations in 1998. The inset shows the variation of refractivity as function of height. The unpredictable wet part of the refractivity accounts for most of the variability.

possible to derive the statistics of delay differences between two points for every height interval. Using ERS orbit characteristics, the 2σ values and worst-case values for a 1 day interval and a 182 days interval are shown in Fig. 4. With an accu-

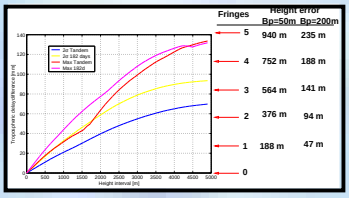

Fig. 4. Error due to vertical stratification.

racy better than 2–3 mm we find the following empirical model for the standard deviation of the interferometric phase due to differential tropospheric layering:

$$\sigma_\varphi = \frac{4\pi}{\lambda\cos\theta}(33.7 + 0.08\Delta t)\sin\frac{h\pi}{2h_s}, \qquad (7)$$
$$\text{for} \quad 1 \le \Delta t \le 182, \quad \text{and} \quad 0 \le h \le h_s$$

where Δt is the time interval in days, h represents height in m, and $h_s = 5000$ m is a scale height. Above this height the variability of the refractivity is considered negligible.

2.2 Error due to turbulent mixing

The effect of turbulent mixing, resulting in 3D spatial heterogeneity of refractivity, is an even more general form of atmospheric disturbance, affecting all types of space-geodetic radio observations (VLBI, GPS, INSAR). On short spatial scales the dominant signal is caused especially by water vapor variability. Fig. 5 shows the power law behavior of the turbulent signal. A $-8/3$ exponent is generally accepted to describe the variability. The insets show the corresponding differential interferograms.

The power spectra curves are obtained using a rotational average over the 2D spectrum. The variance of phase difference

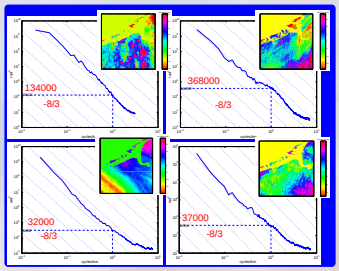

Fig. 5. Atmospheric power spectra of four arbitrary interferograms.

measurements over a fixed spatial interval is found using the structure function:

$$D_\varphi(R) = E\{[\varphi(x+R) - \varphi(x)]^2\}, \qquad (1)$$

as shown in Fig. 6. The empirically found structure functions

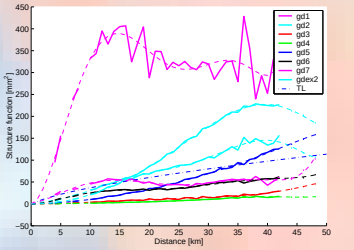

Fig. 6. Structure functions $D_\varphi(R)$ of eight 'atmospheric' interferograms. The structure function is an expression for the variance of a spatial difference.

$D_\varphi(R)$ can be used to derive the covariance function:

$$Cov(i,j) = \frac{1}{2}\{D_\varphi(\infty) - D_\varphi(R)\}, \qquad (8)$$

and expanding this covariance function for all the combinations of pixel i and j yields the variance covariance matrix $\mathbf{C}_{\mathbf{s}}$, as shown in Fig. 7. Note that $\mathbf{C}_{\mathbf{s}}$ is a Block Toeplitz-Toeplitz

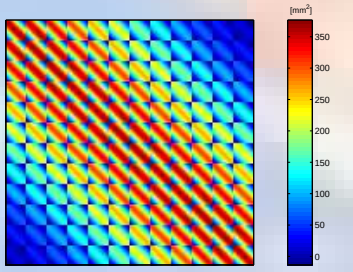

Fig. 7. Variance covariance matrix $\mathbf{C}_{\mathbf{s}}$ derived from the empirical structure function.

Block (BTTB) matrix. For these matrix forms, fast inversion techniques exist.

3. Conclusions

For applications of repeat-pass radar interferometry, atmospheric signal needs to be included in the mathematical model. As long as no effective means are available to obtain quantitative information with sufficient spatial resolution, high accuracy, and at the time of the SAR acquisitions, the atmospheric signal will deteriorate the quality of the topographic map or deformation model. Hence, it is necessary to describe the error in a more stochastic sense, and include it in the dispersion of the observations.